

Scattering of excitons by long-wavelength magnons in the quasi-one-dimensional antiferromagnet $\text{CsMnCl}_3 \cdot 2\text{H}_2\text{O}$

V. V. Eremenko, I. S. Kachur, V. P. Novikov, and V. V. Shapiro

Low Temperature Physicotechnical Institute, Ukrainian Academy of Sciences

(Submitted 3 February 1988)

Zh. Eksp. Teor. Fiz. **94**, 225–233 (September 1988)

We have carried out measurements of the half-width of excitonic optical absorption bands in the quasi-one-dimensional antiferromagnetic (AFM) compound $\text{CsMnCl}_3 \cdot 2\text{H}_2\text{O}$ and the three-dimensional antiferromagnet MnF_2 in magnetic fields oriented along the axis of easy magnetization of these crystals. In the AFM phase the exciton band in the quasi-one-dimensional AFM crystal $\text{CsMnCl}_3 \cdot 2\text{H}_2\text{O}$ undergoes a broadening by more than a factor of three for magnetic fields near the critical field H_c of the orientational (spin-flop) phase transition; at the same time, in the three-dimensional MnF_2 the broadening of this band is no more than 10%. The increase in the half-width of the exciton band in the neighborhood of the field H_c is related to scattering of the excitons by the low-frequency branch magnons, whose number increases exponentially as the energy of this branch decreases in the field. The magnitude of the effect depends on the density of states $\rho(\epsilon)$ of the long-wavelength magnons; it is a maximum in one-dimensional crystals, where $\rho(\epsilon)$ has a singularity near the bottom of the spin-wave band. Using Green's-function methods, we have estimated the broadening of the excitonic optical absorption band in these AFM crystals that differ in the dimensionalities of their magnetic structures. We show that in a one-dimensional AFM insulator the exciton-magnon interaction leads to significant broadening of the exciton band in the neighborhood of the critical field H_c .

$\text{CsMnCl}_3 \cdot 2\text{H}_2\text{O}$ crystals are antiferromagnetically ordered at $T_N = 4.89$ K. The peculiarity of the magnetic structure of these crystals lies in the fact that the magnetic Mn^{2+} ions form chains oriented along the direction normally referred to as the a -axis of the orthorhombic unit cell. The exchange integral J within the chains exceeds by two orders of magnitude the exchange integral J^* between chains.¹ This quasi-one-dimensional antiferromagnetic structure gives rise to a singularity in the energy dispersion of spin waves; when the wave vector \mathbf{k} is oriented along the a -axis, the energy varies from ϵ_0 (i.e., the energy of a spin wave at the center of the Brillouin zone, which equals the gap in the spectrum) to ϵ_{max} (the maximum value of the magnon energy, which occurs at the edge of the Brillouin zone, where $ka = \pi/2$), while for directions transverse to the a -axis the energy dispersion is very small. This leads to additional singularities in the energy distribution of the magnon density of states $\rho(\epsilon)$ of a one-dimensional antiferromagnet: besides a peak near the top of the zone, i.e., $\rho(\epsilon_{\text{max}})$, there appears a peak near its bottom, i.e. $\rho(\epsilon_0)$.² Recently³ it was shown that a high magnon density of states near the bottom of a band gives rise to singularities in the exciton-magnon optical absorption in the quasi-one-dimensional AFM $\text{CsMnCl}_3 \cdot 2\text{H}_2\text{O}$.

In this paper we investigate both theoretically and experimentally the width of the excitonic optical absorption band in $\text{CsMnCl}_3 \cdot 2\text{H}_2\text{O}$, and show that singularities in its behavior near the orientational phase transition induced by an external magnetic field—i.e., the overturning of the magnetic sublattices [the “spin-flop” (SF) transition which occurs at $H_c \approx 1.8$ T at a temperature of 1.96 K]—is caused by scattering of excitons by spin waves. A decisive role is played here by the high magnon density of states near the bottom of the band in a quasi-one-dimensional crystal.

EXPERIMENT

In studying the broadening mechanism for optical absorption bands we usually investigate experimentally the

temperature dependence of the band half-widths δ_T .⁴ However, in devising such experiments it is difficult to isolate the contributions to the band width caused by interaction of the excitons with magnons from those due to interactions of the excitons with acoustic phonons. In order to separate out the magnon contribution, we kept the temperature constant while varying the number of thermally-excited magnons by changing the gap ϵ_0 in the spin-wave spectrum. This is most easily accomplished by using an external field \mathbf{H} : if this field is oriented along the easy-magnetization axis, i.e., along the direction of spontaneous magnetic ordering, then the gap ϵ_0 in the lower branch of the spin-wave spectrum decreases practically to zero at a field H_c (see, e.g., Ref. 5). This method of thermally activating magnons—by “softening” the low-frequency spin-wave mode with an external field—possesses more energy selectivity in generating magnon populations than the usual method of raising the temperature. For one and the same value of the magnon occupation number near the top of the band it ensures a very much higher level of population in the neighborhood of the bottom of the band. This feature turns out to be important in calculating the role of the dimensionality of the magnetic structure in AFM crystals, because it is very near the bottom of the magnon band where the energy distributions of the density of magnon states in $1d$ and $3d$ AFMs differ the most. In order to decrease the energy of the spin-wave mode, the magnetic field is applied to $\text{CsMnCl}_3 \cdot 2\text{H}_2\text{O}$ along the b -axis of the orthorhombic structure; in MnF_2 it is applied along the tetragonal C_4 axis.

In order to weaken the effect of phonons on the width of the absorption band, the temperature at which the measurements were made was chosen as far as possible to be on the low side; in $\text{CsMnCl}_3 \cdot 2\text{H}_2\text{O}$ this was 1.96 K. For comparing the behavior of the excitonic-band half-widths of $\text{CsMnCl}_3 \cdot 2\text{H}_2\text{O}$ and MnF_2 , it is convenient to make the ratios of the gaps ϵ_0 in the magnon spectra of the two crystals to the temperatures at which their optical spectra are recorded

close to one another. For this choice of temperatures the occupation numbers n_k of magnons near the bottom of the band are roughly equal in both cases, which makes it easier to compare the experimental results; the common scale used for comparison is the ratio of the external field intensities to the critical value of the field for the spin-flop (SF) transition, i.e., the quantity H/H_c . The temperature $T = 1.96$ K of the $\text{CsMnCl}_3 \cdot 2\text{H}_2\text{O}$ sample corresponds in the above sense to a temperature $T \approx 10$ K for MnF_2 . In practice our measurements on MnF_2 were made at the somewhat higher temperature $T = 14$ K.

Thus, the experiment reduces to measurement of the half-width of the exciton optical absorption band as a function of the intensity of the external magnetic field for $\mathbf{H} \parallel b$ ($\text{CsMnCl}_3 \cdot 2\text{H}_2\text{O}$) and $\mathbf{H} \parallel C_4$ (MnF_2).

The spectrometer we chose for our measurements was a DFS-13 diffraction spectrograph with a linear dispersion 2 \AA/mm . The spectra were recorded both by the usual photographic method with a subsequent photometric analysis and by using an optical multichannel analyzer (a 1450A system from the Princeton Applied Research company).

Magnetic field intensities of up to 8 T were generated using a superconducting solenoid; higher-intensity fields were created using a pulse technique implemented with a capacitor bank. In the latter case only the photographic method was used to record the spectra.^{6,7}

The superconducting solenoid was immersed along with the sample in liquid He^4 , whose vapor pressure was varied by pumping. The sample temperature was monitored by the saturation pressure of the He^4 vapor to an accuracy of 5 mK. To increase the accuracy of our field calibration we used as a reference mark the value of the critical field H_c for the SF transition in $\text{CsMnCl}_3 \cdot 2\text{H}_2\text{O}$, borrowed from the literature data.⁸ Our error in determining field intensities was no worse than 0.1%, which is on the order of the calculated inhomogeneity of the magnetic field at the ends of the sample. The error in determining the magnetic field intensity in the pulsed solenoid came to 1%. We determined the frequencies at which the in-band absorptions were maximal with an accuracy of about 10% of the band half-widths, i.e., 0.1 to 0.3 cm^{-1} for $\text{CsMnCl}_3 \cdot 2\text{H}_2\text{O}$. The error in determining the half-width of the exciton band was 0.03 to 0.1 cm^{-1} for the

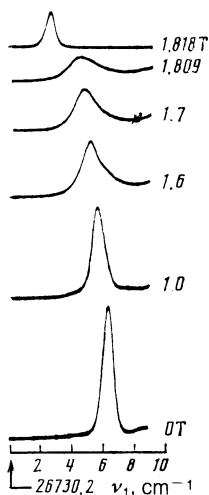


FIG. 1. Broadening of the exciton band for the 26736.7 cm^{-1} transition ${}^6A_{1g}({}^6S) \rightarrow {}^4T_{2g}({}^4D)$ in antiferromagnetic $\text{CsMnCl}_3 \cdot 2\text{H}_2\text{O}$ in the vicinity of the SF transition: $\mathbf{H} \parallel b$, $T = 1.96$ K.

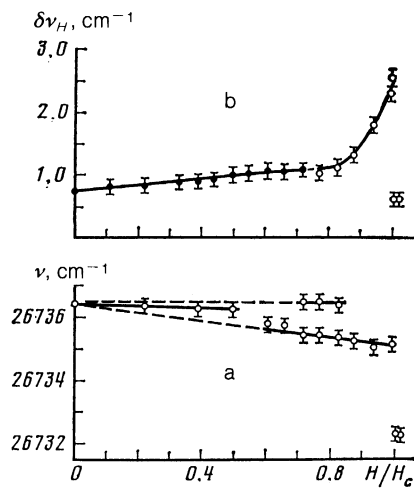


FIG. 2. (a) Measurement of the doublet pseudo-splitting of the exciton band. (b) Dependence of the half-width of the low-frequency component of the doublet on the external magnetic field intensity (light points) in $\text{CsMnCl}_3 \cdot 2\text{H}_2\text{O}$ (the dark points denote the results of measurements of the half-width of the unresolved spectral components of the doublet) at $T = 1.96$ K.

band in $\text{CsMnCl}_3 \cdot 2\text{H}_2\text{O}$ and 0.2 to 0.3 cm^{-1} for the band in MnF_2 .

EXPERIMENTAL RESULTS

We studied the following bands: in $\text{CsMnCl}_3 \cdot 2\text{H}_2\text{O}$ crystals, the exciton band of the ${}^6A_{1g}({}^6S) \rightarrow {}^4T_{2g}({}^4D)$ transition at a temperature 1.96 K in a field $\mathbf{H} \parallel b$; in the crystal MnF_2 the exciton band of the ${}^6A_{1g}({}^6S) \rightarrow {}^4T_{2g}({}^4P)$ transition at a temperature of 14 K in a field $\mathbf{H} \parallel C_4$. The optical electronic transitions are labeled to accord with the irreducible representations of the O_h group, since in both crystals the basic component of the crystal field has cubic symmetry. We denote in parentheses the terms of the free Mn^{2+} ion. In both crystals the sharpest bands in the absorption spectrum were chosen in order to determine the half-widths of these bands more accurately.

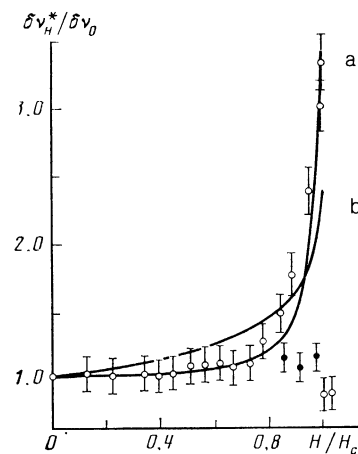


FIG. 3. Dependence of the relative broadening of the exciton bands in $\text{CsMnCl}_3 \cdot 2\text{H}_2\text{O}$ (\circ) and MnF_2 (\bullet) caused by scattering of excitons by spin waves on the magnetic field intensity $\mathbf{H} \parallel b$ for $T = 1.96$ K for $\text{CsMnCl}_3 \cdot 2\text{H}_2\text{O}$ and $\mathbf{H} \parallel C_4$ for $T = 14$ K for MnF_2 . The solid curves are calculations: (a) for a one-dimensional AFM, and (b) for a two-dimensional AFM.

In Fig. 1 we show for the exciton-band profiles for the 1d AFM crystal $\text{CsMnCl}_3 \cdot 2\text{H}_2\text{O}$; the initial one ($H=0$) and in magnetic fields somewhat smaller and somewhat larger than the critical field value H_c .

In Fig. 2b we show the dependence of the half-width of the exciton band in $\text{CsMnCl}_3 \cdot 2\text{H}_2\text{O}$ on the magnetic field intensity when the field is oriented along the easy magnetization axis b of the crystal. In the case of manganese fluoride the half-width of the exciton band increases in fields $H \lesssim H_c$ by approximately 10% compared to its original value, while in the case of $\text{CsMnCl}_3 \cdot 2\text{H}_2\text{O}$ the band widens near the field H_c by roughly a factor of 3.5 (Fig. 3). In the SF phase ($H \gtrsim H_c$) the half-width of the exciton band in $\text{CsMnCl}_3 \cdot 2\text{H}_2\text{O}$ returns to its original value in the absence of an external magnetic field; for MnF_2 in fields $H \gtrsim H_c$ no significant changes are observed in the half-width of the band compared to its value for $H \lesssim H_c$.

THEORY

We are interested in exciton-band broadening due to scattering of excitons by spin waves. Therefore it is necessary to include in the energy operator for excitons the exciton-magnon interaction responsible for this scattering. In the lattice representation the interaction between electrons and spin excitations is described by the expression

$$H_{e-m} = \sum_{\mathbf{n}, \alpha, a} [(J'S'_{n\alpha} S_{n\alpha+\Delta_a} - JS_{n\alpha} S_{n\alpha+\Delta_a}) B_{n\alpha}^+ B_{n\alpha} + (J'S'_{n\alpha} S'_{n\alpha+\Delta_a} - JS_{n\alpha} S_{n\alpha+\Delta_a}) B_{n\alpha+\Delta_a}^+ B_{n\alpha+\Delta_a}]. \quad (1)$$

Here \mathbf{n} is a site vector of the crystal lattice, and α numbers the magnetic sublattices. For simplicity we will assume that the magnetic system $\text{CsMnCl}_3 \cdot 2\text{H}_2\text{O}$ is a two-sublattice system, and designate each sublattice by the direction of its equilibrium magnetization, $\alpha = 1$ and 2, J' and S' are respectively the exchange integral and spin under photoexcitation, while J and S correspond to the ground state, Δ_a is a radius vector connecting a magnetic ion with one of its nearest neighbors a belonging to the other sublattice, and $B_{n\alpha}^+$ and $B_{n\alpha}$ are creation and annihilation operators for electron excitations at the site $n\alpha$.

We will limit our investigation to the low-frequency spin-wave branch only, because the majority of thermally-excited magnons belong to this branch; therefore these magnons essentially determine the scattering of the excitons. In addition, in our later estimates we will neglect the biaxiality of the AFM crystal $\text{CsMnCl}_3 \cdot 2\text{H}_2\text{O}$. This is a completely valid assumption if we are interested only in the behavior of the energy gap ε_0 in the spin-wave spectrum for fields near the critical value of the field H_c oriented exactly along the b -axis.

Introducing the parameters

$$\varphi = \frac{J'}{J} \left(\frac{S'}{S} \right)^{1/2} - 1, \quad \rho = \frac{J'S'}{JS} - 1, \quad e = \frac{J'}{J} - 1$$

and carrying out the Holstein-Primakoff transformation along with a u - v and Fourier transformation, we obtain an expression for the exciton-magnon interaction operator:

$$H_{e-m, \mu} = \frac{JSz}{N} \sum_{\mathbf{k}_1, \dots, \mathbf{k}_3} [\Phi_{1\mu}(\mathbf{k}_2, \mathbf{k}_3) B_{\mu}^+(\mathbf{k}_1 - \mathbf{k}_2 + \mathbf{k}_3) \times B_{\mu}(\mathbf{k}_1) b^+(\mathbf{k}_2) b(\mathbf{k}_3) + \Phi_{2\mu}(\mathbf{k}_2, \mathbf{k}_3) B_{\mu}^+(\mathbf{k}_1 + \mathbf{k}_2 - \mathbf{k}_3) B_{\mu}(\mathbf{k}_1) b(\mathbf{k}_2) b^+(\mathbf{k}_3)], \quad (2)$$

where $B_{\mu}^+(\mathbf{k})$ and $B_{\mu}(\mathbf{k})$ are operators for creation and annihilation of excitons in the μ th band, while $b^+(\mathbf{k})$ and $b(\mathbf{k})$ are the same for the low-frequency magnon branch; N is the number of sites in the crystal lattice; z is the number of nearest magnetic neighbors from the opposite sublattice, so that in this case $z = 2$. The subscript μ indicates the exciton band; for definiteness $\mu = 1$ will refer to the low-frequency band and $\mu = 2$ to the high-frequency bands.

The interaction amplitudes $\Phi_{i\mu}$ have the form

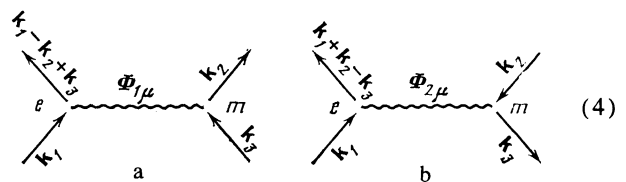
$$\begin{aligned} \Phi_{11}(\mathbf{k}_2, \mathbf{k}_3) &= -\varphi v_{\mathbf{k}_2} u_{\mathbf{k}_3} \gamma_{\mathbf{k}_2} + e u_{\mathbf{k}_2} u_{\mathbf{k}_3}, \\ \Phi_{12}(\mathbf{k}_2, \mathbf{k}_3) &= -\varphi v_{\mathbf{k}_2} u_{\mathbf{k}_3} \gamma_{\mathbf{k}_2} + \rho u_{\mathbf{k}_2} u_{\mathbf{k}_3} \gamma_{\mathbf{k}_2 - \mathbf{k}_3}, \\ \Phi_{21}(\mathbf{k}_2, \mathbf{k}_3) &= -\varphi v_{\mathbf{k}_2} u_{\mathbf{k}_3} \gamma_{\mathbf{k}_2} + \rho v_{\mathbf{k}_2} v_{\mathbf{k}_3} \gamma_{\mathbf{k}_2 - \mathbf{k}_3}, \\ \Phi_{22}(\mathbf{k}_2, \mathbf{k}_3) &= -\varphi v_{\mathbf{k}_2} u_{\mathbf{k}_3} \gamma_{\mathbf{k}_2} + e v_{\mathbf{k}_2} v_{\mathbf{k}_3}. \end{aligned} \quad (3)$$

Here $u_{\mathbf{k}}$ and $v_{\mathbf{k}}$ are the coefficients of the Bogolyubov-Tyablikov u - v transformation. Their specific forms for a uniaxial AFM with easy-axis anisotropy are given, e.g., in Refs. 9 and 10:

$$\gamma_{\mathbf{k}} = \frac{1}{z} \sum_a \exp(i\mathbf{k}\Delta_a)$$

where the summation extends over nearest neighbors from the opposite sublattice.

The terms in Eq. (2) can be associated with the following diagrams:



Here the letters e and m denote respectively exciton and magnon lines; their interactions of amplitudes $\Phi_{i\mu}$ are shown as wavy lines. The diagrams in (4) correspond to scattering processes which preserve the number of particles.

The operator for the exciton-magnon interaction (2) in a collinear AFM, in contrast to a noncollinear AFM, does not contain any odd powers of the creation and annihilation operators for magnons and is a bilinear function of them. This follows directly from the Heisenberg form of the operator (1) in terms of the spin operators S and S' , a form that reflects the conservation law for spin projections in the exciton-magnon scattering processes.

The form we have obtained for the exciton-magnon interaction operator (2) is structurally equivalent to that of the exciton-phonon interaction operator, when the latter is quadratic in the creation and annihilation operators for phonons.¹¹ The individual characteristics of the interaction between excitons and magnons depend on the specific form of the interaction amplitudes $\Phi_{i\mu}$ (3). Therefore, in order to solve the problem of scattering of excitons by spin waves we can use (with some insignificant changes) a method used in investigations of scattering of excitons by phonons.¹¹

The form of a pure exciton absorption band is described using the single-particle exciton Green's function.¹² Let us introduce the retarded Green's function

$$G_{\mu\mu'}(\mathbf{k}, t) = -i\theta(t) \langle\langle B_{\mu}(\mathbf{k}, t) B_{\mu'}^{\dagger}(\mathbf{k}, 0) \rangle\rangle, \quad (5)$$

where $\theta(t)$ is a step function in the time t ; $B_{\mu}^{\dagger}(\mathbf{k}, t)$ and $B_{\mu}(\mathbf{k}, t)$ are operators for creation and annihilation of excitons in the Heisenberg representation, $\langle\langle \dots \rangle\rangle$ denotes a Gibbs average. The Fourier transformation to the energy representation gives:

$$G_{\mu\mu'}(\mathbf{k}, \omega) = \frac{1}{2\pi} \int_{-\infty}^{\infty} e^{i\omega t} G_{\mu\mu'}(\mathbf{k}, t) dt. \quad (6)$$

The exciton Green's function in the absence of interactions with magnons ($H_{e-m} = 0$) has the form ($\delta \rightarrow 0$):

$$G_{\mu\mu'}^{(0)}(\mathbf{k}, \omega) = \frac{\delta_{\mu\mu'}}{\omega - \hbar^{-1} E_{e,\mu}(\mathbf{k}) + i\delta} \equiv G_{\mu}^{(0)}(\mathbf{k}, \omega), \quad (7)$$

where $E_{e,\mu}(\mathbf{k})$ is the exciton energy dispersion.

When we take into account the exciton-magnon interaction, the Green's function (6) is represented as an infinite series in terms of the "zero-order" functions (7). Let us represent this expansion in the form of Feynman diagrams:

$$\text{Thick line} = \text{Thin line} + \text{Thin line with magnon loop} + \text{Thin line with two magnon lines} + \text{Thin line with magnon loop and magnon line} + \dots \quad (8)$$

Here the solid lines correspond to Green's functions for excitons [the thick lines are the sought Green's function (6), and the thin ones are the zero-order functions (7)], while the dashed lines denote magnon lines. These latter should be furnished with arrows; in these diagrams it is necessary to carry out an additional summation (left-hand arrow, right-hand arrow). A factor $n_{\mathbf{k}} + 1$ is associated with each magnon line carrying an arrow from left to right, while a factor $n_{\mathbf{k}}$ goes with lines whose arrows go from right to left. Here

$$n_{\mathbf{k}} = \left[\exp\left(\frac{\varepsilon_{\mathbf{k}} - \mu_B g H}{k_B T}\right) - 1 \right]^{-1}$$

is the occupation number for magnons,

$$\varepsilon_{\mathbf{k}} = \varepsilon_{\max} (1 + 2\beta^2 - \gamma_{\mathbf{k}}^2)^{1/2}$$

is their energy dispersion in the absence of the field, $\varepsilon_{\max} = JSz$ is the maximum energy of a spin wave at the Brillouin zone boundary at the point $k_x = \pi/2a$ ($x||a$), $\beta = \varepsilon_0/\varepsilon_{\max}$, ε_0 is the energy gap in the magnon spectrum, μ_B is the Bohr magneton, g is the spectroscopic splitting factor (here $g = 2$), and k_B is Boltzmann's constant. At each vertex, which is denoted by a point, two exciton and two magnon lines come together; the interaction events (4) occur at these vertices. The vertices marked with crosses are associated with the quantity $2\pi A_{\mu}$, where

$$A_{\mu} = \frac{\varepsilon_{\max}}{N} \sum_{\mathbf{k}_2} [\Phi_{1\mu}(\mathbf{k}_2, \mathbf{k}_2) n_{\mathbf{k}_2} + \Phi_{2\mu}(\mathbf{k}_2, \mathbf{k}_2) (n_{\mathbf{k}_2} + 1)].$$

Only exciton lines enter and exit these crossed vertices; the interaction is with virtual magnons.

In general it is impossible to sum the series (8). An approximate value for the Green's function can be obtained by terminating the series after calculating the exciton mass operator $M(\mathbf{k}, \omega)$ to a given order of perturbation theory.¹² However, this method is hardly applicable in the present case, since we are obliged then to limit ourselves to a small number of interaction events (3). In the vicinity of the field H_c (i.e., near the SF transition), however, when the number of thermally-excited magnons begins to increase significantly, the necessity arises for including multistep exciton-magnon scattering events. Therefore, in order to calculate approximately the exciton Green's function (8), we will make use of the fact that in the neighborhood of H_c the energy of the low-frequency spin-wave branch becomes significantly smaller than the half-width of the exciton band. It is found that if we neglect magnon frequencies compared to the frequency detuning in the denominators of the zero-order Green's functions of the expansion (8), then we can sum the full series (8) just as for the case of exciton-phonon interactions.¹¹

Introducing

$$L_{\mu} = (\varepsilon_{\max}/N)^2 \sum_{\mathbf{k}_2, \mathbf{k}_3} [|\Phi_{1\mu}(\mathbf{k}_2, \mathbf{k}_3)|^2 (n_{\mathbf{k}_3} + 1) n_{\mathbf{k}_2} + |\Phi_{2\mu}(\mathbf{k}_2, \mathbf{k}_3)|^2 (n_{\mathbf{k}_2} + 1) n_{\mathbf{k}_3}]$$

and assuming, as was done in Ref. 11, that $A_{\mu} \approx L_{\mu}^{1/2} \ll |\hbar\omega - E_{e\mu}|$, we have

$$G_{\mu}(\mathbf{k}, \omega) = G_{\mu}^{(0)}(\mathbf{k}, \omega) + \sum_{n=1}^{\infty} 1 \cdot 3 \cdot 5 \cdot 7 \dots (2n-1) \times (2\pi A_{\mu})^n [G_{\mu}^{(0)}(\mathbf{k}, \omega)]^{n+1}. \quad (9)$$

We assume that the exciton state is nondispersive. In a one-dimensional structure with interchain antiferromagnetic ordering the exchange interaction between ions with parallel-oriented spins is usually small, while the dispersion of an exciton in a collinear AFM is determined in the Heitler-London approximation by precisely this interaction with the ferromagnetic neighbors.¹⁰

The series (9) can be summed; the quantity A_{μ} determines the half width of the exciton band.

Using the equations in (3), we obtain the following expression for A_1 :

$$A_1 = A_1^0 + A_1(H),$$

$$A_1^0 = \varepsilon_{\max} a \int_0^{\pi/2a} \frac{\rho(\varepsilon_{\max} - \varepsilon_{\mathbf{k}}) - \varphi \varepsilon_{\max} \gamma_{\mathbf{k}}^2}{\varepsilon_{\mathbf{k}}} d\mathbf{k}, \quad (10)$$

$$A_1(H) = \varepsilon_{\max} a \int_0^{\pi/2a} \frac{\rho(\varepsilon_{\max} - \varepsilon_{\mathbf{k}}) + e(\varepsilon_{\max} + \varepsilon_{\mathbf{k}}) - 2\varphi \varepsilon_{\max} \gamma_{\mathbf{k}}^2}{\varepsilon_{\mathbf{k}}} n_{\mathbf{k}} d\mathbf{k},$$

where a is the spacing between neighboring magnetic neighbors from the opposite sublattice. The quasimomentum \mathbf{k} loses its vector character in the one-dimensional case.

The expressions for A_2^0 and $A_2(H)$ are obtained from (10) by making the replacement $\rho \rightleftharpoons e$.

In the immediate vicinity of H_c the basic contribution to $A_{\mu}(H)$ comes from magnons with $k \approx 0$. In this case

$$A_{\mu}(H) \sim (1 - H/H_c)^{-1}. \quad (11)$$

Equation (11) reveals a strong divergence in the dependence of the exciton band half-width in a one-dimensional AFM crystal on the magnetic field intensity in the vicinity of the critical field H_c .

An analogous estimate made for two-dimensional AFMs gives a weaker divergence:

$$A_{\mu}(H) \sim -\ln(1 - H/H_c). \quad (12)$$

In a three-dimensional AFM crystal the quantity $A_{\mu}(H)$ has a finite limit near the field H_c .

Let us note that if we include subtler interactions in the discussion, for example magnetoelastic interactions, the increase in the half-width of the exciton band described by Eqs. (11) and (12) near the SF transition is no longer unbounded. In addition, in the immediate vicinity of the field H_c , when the number of occupied magnons $n_k \gtrsim 1$, the spin-wave approximation we have used becomes incorrect. In this sense, the estimates (11) and (12) must be viewed as determining a trend leading to broadening of the optical absorption bands in AFM crystals whose magnetic structures have various dimensionalities.

DISCUSSION

In order to compare the experimental and calculated results it is necessary to extract from the experimental dependence of the exciton band half-width that part which can be related to exciton-magnon scattering. The broadening of the band (Fig. 2b) in the magnetic field interval $0 < H < 0.77 H_c$, i.e., $H < 1.4$ T, is related to a Zeeman pseudosplitting of the AFM sublattices which is unresolved in such weak fields. In this field interval, where the components of the doublet are not yet resolved, we measured the total half-width of the band profile (Fig. 2b—the dark points). In magnetic fields above 1.4 T the band clearly splits into a doublet. Therefore in these fields we show on the graph the half width of the (more intense) low-frequency component of the doublet (the light points).

Thus, in the case of $\text{CsMnCl}_3 \cdot 2\text{H}_2\text{O}$, in order to compare with calculations it is necessary to exclude the exciton-band broadening caused by this sublattice splitting. Figure 3 illustrates the ratio $\delta v_H^*/\delta v_0$ of the half-width of the exciton band in a magnetic field to the half-width of this band in the absence of the field. Here, δv_0 is the initial half-width of the band; for small broadening, the half-width δv_H^* differs from δv_H by a correction associated with the sublattice splitting. This broadening can be approximated by a linear dependence $\delta v(H) = \delta v_0 + \alpha H$, and all the values of the half-width δv_H^* in the region 0–1.4 K are decreased by the quantity αH compared to δv_H . By plotting the function $\delta v_H^*/\delta v_0$, we exclude the contribution from the exciton-phonon scattering mechanism assuming additivity of the magnon and phonon contributions to the bandwidth. On this figure the analogous ratios of half widths are shown also for the exciton band in the spectrum of manganese fluoride (the dark points). In addition, the experimental $\delta v_H^*/\delta v_0$ dependence for absorption band of $\text{CsMnCl}_3 \cdot 2\text{H}_2\text{O}$ are compared with the theoretical estimates (11) and (12), which are obtained for one-dimensional and three-dimensional AFM crystals, respectively. The experimental points are close enough to the calculated curve (11), though some deviation is ob-

served in the immediate vicinity of H_c . Apparently the experimental data are concentrated between curves (11) and (12); however, for the most part they are biased toward the function (11) which corresponds to the one-dimensional AFM crystal.

CONCLUSION

1. We have experimentally investigated the dependence of the half width of the exciton bands of the quasi-one-dimensional AFM insulator $\text{CsMnCl}_3 \cdot 2\text{H}_2\text{O}$ and the three-dimensional AFM MnF_2 on the magnetic field intensity at a fixed temperature considerably lower than the Debye temperature ($T \ll \Theta_D$) and rather low compared to the Néel temperature ($T \approx 1/3 T_N$).

2. It was observed that as the field intensity increases in the antiferromagnetic phase of the crystal $\text{CsMnCl}_3 \cdot 2\text{H}_2\text{O}$ a strong broadening of the exciton band occurs near the critical value H_c of the field for the SF transition (in the interval $0.8H_c < H < H_c$).

3. The half-width of the exciton band for a three-dimensional AFM crystal is practically independent of magnetic field intensity either for the antiferromagnetic or the SF phase.

4. We have presented an estimate of the width of the exciton optical absorption band within the context of a theory of scattering of excitons by spin waves based on the use of Green's functions. We have shown that in a one-dimensional AFM insulator the exciton-magnon interaction leads to a significant broadening of the exciton band with increasing field intensity near the critical field H_c . This effect is connected with the presence of a peak in the density of magnon states $\rho(\varepsilon)$ near the bottom of the magnon band. The decrease in the energy of the bottom of this band in the vicinity of the SF transition leads to an increase in the number of thermally excited magnons, and correspondingly to a broadening of the optical absorption band. In the SF phase the energy of the bottom of the magnon band increases discontinuously, as a result of which the broadening of the exciton band decreases.

In the three-dimensional AFM crystal MnF_2 there is no peak in the density of states near the bottom of the magnon band. For this reason, there is a complete absence of broadening of the exciton band for this crystal in a magnetic field.

¹H. Nishihara, W. J. M. de Jonge, and T. de Neef, *Phys. Rev.* **B12**, 5325 (1975).

²W. J. M. de Jonge, K. Kopinga, and C. H. W. Swuste, *Phys. Rev.* **B14**, 2137 (1976).

³V. P. Novikov, I. S. Kachur, and V. V. Eremenko, *Fiz. Nizk. Temp.* **7**, 223 (1981) [*Sov. J. Low Temp. Phys.* **7**, 108 (1981)].

⁴W. M. Yen, G. M. Imbush, and D. L. Huber, *Optical Properties of Ions in Crystals* (New York-London-Sydney: Interscience, 1967), p. 301.

⁵A. G. Anders, A. I. Zvyagin, and A. I. Petutin, *Fiz. Nizk. Temp.* **3**, 649 (1977) [*Sov. J. Low Temp. Phys.* **3**, 316 (1977)].

⁶P. L. Kapitza, P. G. Strelkov, and E. Ya. Lauerman, *Zh. Eksp. Teor. Fiz.* **8**, 276 (1938).

⁷V. V. Eremenko and Yu. A. Popkov, *Ukr. Fiz. Zh.* **8**, 88 (1963).

⁸A. C. Botterman, W. J. M. de Jonge, and P. de Leeuw, *Phys. Lett.* **A30**, 150 (1969).

⁹J. B. Parkinson and R. Loudon, *J. Phys.* **C1**, 1568 (1968).

¹⁰V. V. Eremenko, Introduction to the Optical Spectroscopy of Magnets [in Russian], Kiev: Nauk, Dumka, 1975.

¹¹V. M. Agranovich, Theory of Excitons [in Russian], Moscow: Nauka, 1968.

¹²A. S. Davydov, Theory of Molecular Excitons [in Russian], Moscow: Nauka, 1968.

Translated by F. Crowne